

# B2114+022: a distant radio source gravitationally lensed by a starburst galaxy

Pedro Augusto,<sup>1,2,†</sup> Ian W. A. Browne,<sup>1,★</sup> Peter N. Wilkinson,<sup>1</sup> Neal J. Jackson,<sup>1</sup>  
Chris D. Fassnacht,<sup>3,‡</sup> Tom W. B. Muxlow,<sup>1</sup> Jens Hjorth,<sup>4</sup> Andreas O. Jaunsen,<sup>4</sup>  
Leon V. Koopmans,<sup>1,5</sup> Alok R. Patnaik<sup>1,6</sup> and Greg B. Taylor<sup>3</sup>

<sup>1</sup>*University of Manchester, Jodrell Bank Observatory, Macclesfield, Cheshire SK11 9DL*

<sup>2</sup>*Centro de Astrofísica da Universidade do Porto, Rua do Campo Alegre, 823, 4150 Porto, Portugal*

<sup>3</sup>*National Radio Astronomy Observatory, PO Box O, Socorro, New Mexico 87801, USA*

<sup>4</sup>*University of Copenhagen, Astronomical Observatory, Juliane Maries Vej 30, 2100 Copenhagen 0, Denmark*

<sup>5</sup>*California Institute of Technology, Pasadena, CA 91125, USA*

<sup>6</sup>*Max Planck Institute für Radioastronomie, Auf dem Hügel 69, D-53121 Bonn, Germany*

Accepted 2001 June 13. Received 2001 June 13; in original form 2000 December 21

## ABSTRACT

We have discovered a radio source (B2114+022) with a unique structure during the course of the JVAS gravitational lens survey. VLA, MERLIN, VLBA and MERLIN+EVN radio maps reveal four compact components, in a configuration unlike that of any known lens system, or, for that matter, any of the  $\sim 15\,000$  radio sources in the JVAS and CLASS surveys. Three of the components are within 0.3 arcsec of each other while the fourth is separated from the group by 2.4 arcsec. The widest separation pair of components have similar radio structures and spectra. The other pair also have similar properties. This latter pair have spectra which peak at  $\sim 5$  GHz. Their surface brightnesses are much lower than expected for synchrotron self-absorbed components.

Ground-based and *Hubble Space Telescope* optical observations show two galaxies ( $z = 0.3157$  and  $0.5883$ ) separated by 1.25 arcsec. The lower redshift galaxy has a post-starburst spectrum and lies close to, but not coincident with, the compact group of three radio components. No optical or infrared emission is detected from any of the radio components down to  $I = 25$  and  $H = 23$ . We argue that the most likely explanation of the B2114+022 system is that the post-starburst galaxy, assisted by the second galaxy, lenses a distant radio source producing the two wide-separation images. The other two radio components are then associated with the post-starburst galaxy. The combination of the angular sizes of these components, their radio spectra and their location with respect to their host galaxy still remains puzzling.

**Key words:** gravitational lensing – galaxies: individual: B2114+022 – galaxies: starburst.

## 1 INTRODUCTION

The JVAS (Jodrell–VLA Astrometric Survey) is a survey of flat-spectrum radio sources whose primary purpose was to find phase-referencing calibrators for MERLIN (Patnaik et al. 1992a; Browne et al. 1998a; Wilkinson et al. 1998). However, the observations are

also ideal for recognizing sources which possess multiple components or have very complex structure which are candidate gravitational lens systems. All lensing candidates amongst the 2384 JVAS sources were then followed up with MERLIN and VLBI (King et al. 1999; Augusto, Wilkinson & Browne 1998) whose higher resolution allows one to separate the genuine lens systems, which consist of multiple flat-spectrum components, from systems containing a flat-spectrum core and steep-spectrum extended radio emission. Many candidates were also followed up with multi-frequency VLA observations to check if their components had similar spectral indices.

The radio source B2114+022 was the sixth strong candidate

\*E-mail: iwb@jb.man.ac.uk

†Present address: Universidade da Madeira, Dep. Matemática, Largo do Colégio, 9000 Funchal, Portugal.

‡Present address: STScI, 3700 San Martin Drive, Baltimore, MD 21218, USA.

**Table 1.** Journal of the radio and optical observations of B2114+022.

| Telescope           | Observing date | Integration time | Frequency or $\lambda$       | Resolution (arcsec) |
|---------------------|----------------|------------------|------------------------------|---------------------|
| VLA-A               | 1992 Oct 18    | 2 min            | 8.4 GHz                      | 0.2                 |
| VLA-A               | 1995 Aug 8     | 4 min            | 1.5 GHz                      | 1.1                 |
| VLA-A               | 1995 Aug 8     | 2 min            | 8.4 GHz                      | 0.2                 |
| VLA-A               | 1995 Aug 8     | 2 min            | 15.0 GHz                     | 0.11                |
| VLA-A               | 1995 Aug 24    | 2.5 min          | 8.4 GHz                      | 0.2                 |
| VLA-A               | 1995 Aug 24    | 18 min           | 15.0 GHz                     | 0.11                |
| VLA-A               | 1999 Aug 14    | 6 min            | 325 MHz                      | 6                   |
| MERLIN              | 1993 Sep 27    | 11 hrs           | 1.6 GHz                      | 0.18                |
| MERLIN              | 1995 Jun 2     | 11 hrs           | 5.0 GHz                      | 0.05                |
| MERLIN              | 1995 Jun 4     | 1 hr             | 5.0 GHz                      | 0.05                |
| MERLIN              | 1995 Jun 14    | 1 hr             | 5.0 GHz                      | 0.05                |
| MERLIN              | 1996 Dec 26    | 1 hr             | 5.0 GHz                      | 0.05                |
| VLBA                | 1995 Nov 12    | 35 min           | 5.0 GHz                      | 0.003               |
| MERLIN+EVN          | 1997 May 31    | 8 hrs            | 1.6 GHz                      | 0.02                |
| NOT                 | 1996 Aug 10    | 10 min           | <i>I</i> band                | 0.5                 |
| Keck                | 1996 July 31   | 20 min           | <i>K</i> band                | 0.8                 |
| Keck                | 1997 July 26   | 50 min           | 390–890 nm                   | –                   |
| <i>HST</i> (WFPC2)  | 1997 Jul 3     | 1000 s           | 555 nm ( <i>V</i> band)      | 0.05                |
| <i>HST</i> (WFPC2)  | 1997 Jul 3     | 3000 s           | 814 nm ( <i>I</i> band)      | 0.05                |
| <i>HST</i> (NICMOS) | 1997 Aug 28    | 5250 s           | 1.6 $\mu$ m ( <i>H</i> band) | 0.13                |

lens system discovered in JVAS, the others being: B0218+357 (Patnaik et al. 1993), B1030+074 (Xanthopoulos et al. 1998), B1422+231 (Patnaik et al. 1992b), B1938+666 (King et al. 1997) and MG 0414+0534 (Hewitt et al. 1992) which was known previously. Unlike the other objects, which were relatively easy to confirm as lens systems, it has proven exceedingly difficult to reach a clear conclusion about the true nature of the B2114+022 system, though we believe that two of the components are lensed images of each other and the other two are not. In this paper we present the extensive radio and optical follow-up observations made of this lens candidate (Table 1). We discuss a range of scenarios which might account for this strange system. A companion paper (Chae, Mao & Augusto 2001) presents a detailed discussion of possible lens mass models.

## 2 RADIO OBSERVATIONS

All radio interferometer data were processed using the NRAO AIPS package and DIFMAP (Shepherd, Pearson & Taylor 1994) through the standard routines. During the observations we used standard point-source and flux calibrators as well as fringe finders for the VLBI observations and a nearby phase-referencing calibrator for the MERLIN observations.

The initial JVAS 8.4-GHz map (Browne et al. 1998a) showed B2114+022 to have a very unusual structure. It has four compact radio components in a configuration unlike that of any known lensed system or, for that matter, of any other radio source in the JVAS+CLASS (Cosmic Lens All-Sky Survey; e.g. Browne et al. 1998b) data base which contains a total of  $\sim 15\,000$  sources. As shown in the MERLIN 5-GHz map (Fig. 1) three of the components are within 0.3 arcsec of each other and the fourth is  $\sim 2$  arcsec away.

MERLIN+EVN 1.6-GHz observations reveal extended structure in the components of B2114+022; the resultant map is presented in Fig. 2. From this map and the results of model fitting to the visibilities (Table 2), it appears that components A and D have structures dominated by unresolved components  $\leq 10$  milli-arcsec (mas) in size while B and C have no clear compact features

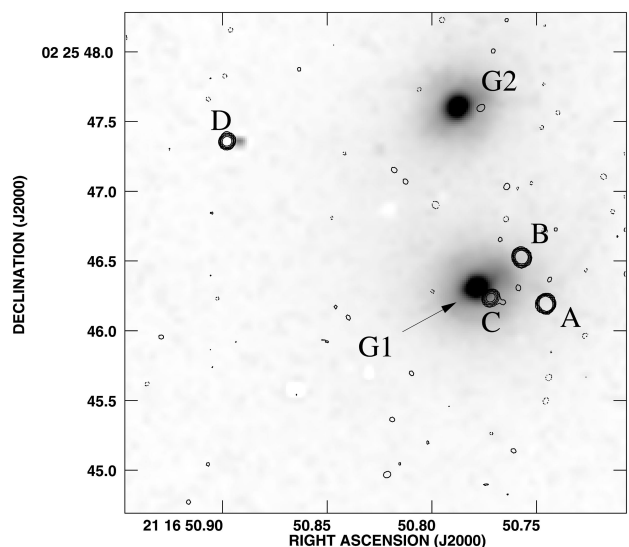


**Figure 1.** 1995 June 2 MERLIN 5-GHz radio map of B2114+022 superimposed on *HST* NICMOS *H*-band image of the field with a relative astrometric accuracy of  $\sim 0.1$  arcsec. G1 is the main lensing galaxy.

and are extended on scales of tens of mas. The sizes of the components are entirely consistent with those seen in a VLBA 5-GHz snapshot observation (Augusto 1996) in which components A and D were easily detected and found to be  $\leq 1$  mas in size, component B was detected with a size of  $\sim 30$  mas while C was resolved out.

Our data taken over several years and at various frequencies (Table 1) allow us to build up spectra for all four components. We see no evidence for variability at  $\geq 10$  per cent level. In Table 3 we present the component radio flux densities measured at various frequencies. The spectra of the components are shown in Fig. 3, together with the overall spectrum for B2114+022 which has a pronounced turnover at  $\sim 3$  GHz. At frequencies below 5 GHz the spectra of components A and D, although similar to each other, are significantly steeper than those of components B and C. The latter

have similar spectra (see Table 3) both peaking around 5 GHz. The steeper spectra of A and D would lead us to expect that they should be more extended than B and C whereas the VLBA 5 GHz (Augusto 1996) and the MERLIN+EVN 1.6 GHz maps show the

**Table 2.** Model fitting for the B2114+022 radio data. We have model fitted separately the 11 h of 5-GHz data taken on 1995 June 2 with MERLIN (M), the 35-min snapshots from the 5-GHz VLBA taken 1995 November 12 (V) and the 8 h of 1.6-GHz data taken with MERLIN+EVN on 1997 May 31 (E). The C component is resolved out in the 5-GHz VLBA data hence the corresponding flux density from model fitting is not presented. For each Gaussian component we give  $S$ , the flux density. The separation vector of each component ( $r, \theta$ ) with respect to A at (J2000) RA 21 16 15.744 Dec. 02 25 46.26 has been derived from the MERLIN 5-GHz data.

| Component     | $S_{5\text{ GHz}}$ (mJy) |    | $S_{1.6\text{ GHz}}$ (mJy) | $r$ (mas)    | $\theta$ ( $^\circ$ ) |
|---------------|--------------------------|----|----------------------------|--------------|-----------------------|
|               | M                        | V  |                            |              |                       |
| A             | 65                       | 44 | 45                         | 0            | 0                     |
| (fuzz near A) |                          |    | $\sim 25$                  |              |                       |
| B             | 52                       | 37 | 28                         | $376 \pm 1$  | $27.79 \pm 0.2$       |
| C             | 16                       | –  | 20                         | $399 \pm 1$  | $83.83 \pm 0.2$       |
| D             | 21                       | 16 | 26                         | $2562 \pm 1$ | $63.14 \pm 0.05$      |

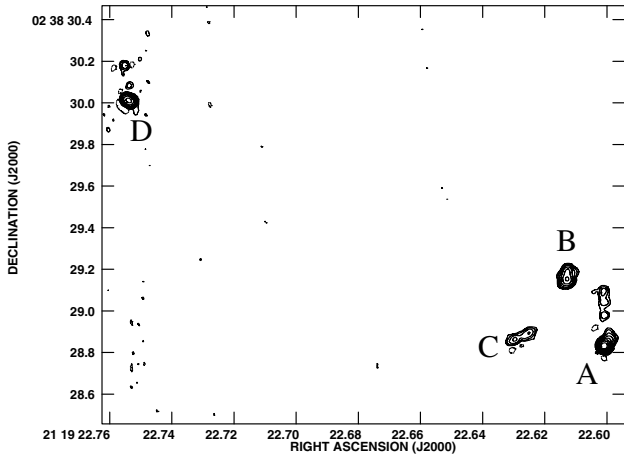


**Figure 2.** The MERLIN+EVN 1.6-GHz map of B2114+022 made from 8 h of observations. The map was restored with a  $30 \times 30$  mas beam and the noise level is  $\sim 75 \mu\text{Jy beam}^{-1}$ . The contour levels start at  $0.17 \text{ mJy beam}^{-1}$  and increase by factors of two reaching a peak of  $38 \text{ mJy beam}^{-1}$ . Component A consists of a compact core and a possible jet-like feature. Component D also has a compact core and some extended structure, the details of which are not well constrained by the current data. Components B and C have no compact cores. The emission to the north of component A is not visible in the MERLIN 5-GHz map and thus if genuine, must have a steep spectrum. The results of model fitting to the components are presented in Table 2.

**Table 3.** The flux densities and spectral indices of the four radio components (A, B, C, D). (The spectral index  $\alpha$  is related to flux density  $S$  and frequency  $\nu$  by  $S \propto \nu^\alpha$ .) The flux densities come from the MERLIN 1.6-GHz observations, the MERLIN 5-GHz observations and VLA 8.4- and 15-GHz observations. The results are plotted in Fig. 3.

| Component | Integrated flux densities (mJy) |              |              |              | Spectral indices     |                       |
|-----------|---------------------------------|--------------|--------------|--------------|----------------------|-----------------------|
|           | 1.6 GHz                         | 5.0 GHz      | 8.4 GHz      | 15.0 GHz     | $\alpha_{1.6}^{5.0}$ | $\alpha_{5.0}^{15.0}$ |
| A         | $73.2 \pm 2$                    | $66.0 \pm 2$ | $38.0 \pm 1$ | $18.8 \pm 1$ | $-0.1 \pm 0.1$       | $-1.1 \pm 0.1$        |
| B         | $32.6 \pm 2$                    | $53.4 \pm 2$ | $36.2 \pm 1$ | $18.5 \pm 1$ | $0.4 \pm 0.1$        | $-1.0 \pm 0.1$        |
| C         | $13.0 \pm 1$                    | $16.1 \pm 1$ | $13.1 \pm 1$ | $6.4 \pm 1$  | $0.2 \pm 0.2$        | $-0.8 \pm 0.3$        |
| D         | $29.6 \pm 1$                    | $20.4 \pm 1$ | $12.5 \pm 1$ | $7.1 \pm 1$  | $-0.3 \pm 0.1$       | $-1.0 \pm 0.3$        |
| Total     | 148                             | 156          | 100          | 51           |                      |                       |

opposite (Fig. 2), with the dominant components of A and D barely resolved while those of B and C are well resolved.

### 3 OPTICAL OBSERVATIONS

#### 3.1 Imaging

On the Palomar Observatory Sky Survey (POSS) there is a magnitude 19 red object within 1 arcsec of the radio centroid of B2114+022. Observations with the NIRC on Keck in 1996 July 31 at  $K$  band, resolve the optical emission into two galaxies with a north-south orientation. *Hubble Space Telescope* (*HST*) observations with WFPC2 were obtained on 1997 July 3 in  $V$  and  $I$  bands and on 1997 August 28 with NICMOS in  $H$  band (Fig. 1, grey-scale). These observations confirmed the presence of the two galaxies which were seen with Keck. The integrated *HST I* magnitudes are  $19.0 \pm 0.1$  for the southern galaxy (G1) and  $19.5 \pm 0.1$  for the northern galaxy (G2). The  $V$  magnitudes are  $20.6 \pm 0.1$  for G1 and  $21.9 \pm 0.1$  for G2. We find  $V - H = 3.6 \pm 0.1$  for G1

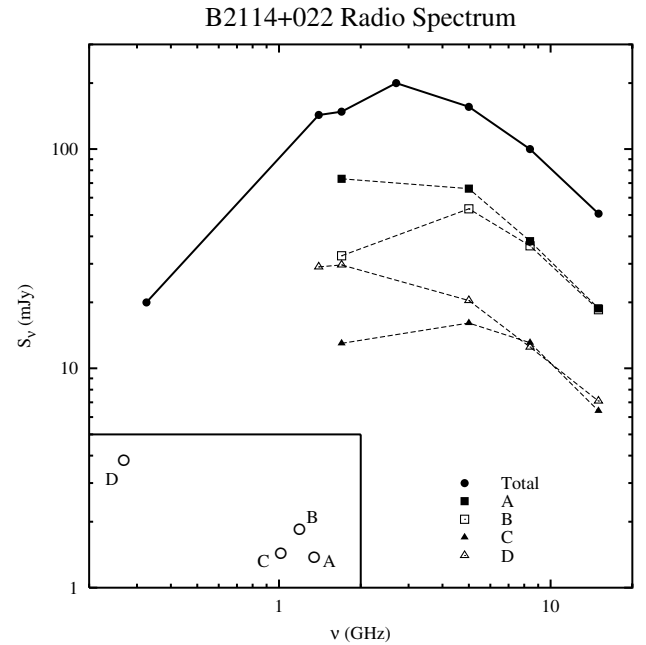


**Figure 3.** Radio spectra for B2114+022 and its components. On top we present the overall spectrum of the B2114+022 system. The detailed spectra of the components are shown below. The integrated flux densities used to construct these spectra come from the 1.6-GHz and 5-GHz MERLIN observations and from VLA observations at 0.325, 1.4, 8.4 and 15 GHz. The 2.7-GHz total flux comes from the Parkes Catalogue.

and  $V - H = 4.6 \pm 0.1$  for G2. These colours are consistent with those expected for early type galaxies at the redshifts we have determined (see below). The position angles of G1 and G2, derived by fitting elliptical isophotes to the light profiles, are  $-80 \pm 10^\circ$  and  $-53 \pm 10^\circ$  respectively. Both galaxies have smooth brightness distributions consistent with them being elliptical galaxies.

Although the potential lensing galaxies G1 and G2 are clearly visible, there is no sign of emission from any of the radio components down to  $I = 25$  and  $H = 23$ .<sup>1</sup> The absence of optical or infrared emission from the radio component D (Fig. 1) is particularly surprising since it is well separated from any contaminating emission or possible absorption associated with G1 and G2.

### 3.2 Spectroscopy

B2114+022 was observed with the Double Spectrograph on the Palomar 200-inch Telescope on 1995 July 23. A 50-min integration on the system produced a spectrum containing an emission line and weak stellar absorption features, suggesting a redshift of  $z \sim 0.316$ . However, the signal-to-noise ratio of the final spectrum was not sufficient to extract redshifts for the two galaxies seen in the optical and infrared images. Thus, the B2114+022 system was re-observed on 1997 July 26 with the Low Resolution Imaging Spectrograph (Oke et al. 1995) on the W. M. Keck II Telescope. The 300 groove  $\text{mm}^{-1}$  grating was used, giving a spectral scale of  $2.44 \text{ \AA pixel}^{-1}$ . The 1.0-arcsec wide slit was aligned at a position angle of  $5^\circ$  to cover the two objects seen in the HST images. Two 1500-s exposures were taken. The data were reduced using standard tasks in IRAF.<sup>2</sup> Observations of the Oke standard star BD+284211 (Oke 1990) were used to correct for the response of the chip. Two objects are clearly seen in the two-dimensional spectra, separated by  $\sim 1.3$  arcsec. The G1 and G2 spectra were extracted from each exposure, weighted by the squares of their signal-to-noise ratios, and then co-added. The final spectra are shown in Fig. 4. Numerous absorption and emission lines are seen in the spectra, providing unambiguous redshifts for G1 and G2,  $z_{G1} = 0.3157 \pm 0.0003$ ,  $z_{G2} = 0.5883 \pm 0.0003$ . The uncertainties in the redshifts are derived from the rms scatter in the redshifts produced by the individual spectral lines. G2 appears to be an elliptical galaxy whereas the G1 spectrum most resembles that of a star-burst galaxy like M82 (Kennicutt 1992). Thus we would classify G2 as an elliptical galaxy and G1 as an ‘E + A’ or a ‘post-starburst galaxy’ (Dressler & Gunn 1983).

### 3.3 Astrometry

A key step towards understanding the B2114+022 system is to establish an accurate registration of the radio and optical images. The positions of the radio components derived from the 1992 VLA 8.4-GHz observations (table 1 of Browne et al. 1998a), are given in Table 4 and have estimated errors  $\leq 20$  mas. These positions agree to within 10 mas of the independent positions derived from VLA 8.4-GHz observations made in 1995 (Table 1).

<sup>1</sup> The faint feature visible in Fig. 1 near the radio component D arises from a single bad pixel which we also see in NICMOS images of the lens systems B1600+434 and MG0414+054.

<sup>2</sup> IRAF (Image Reduction and Analysis Facility) is distributed by the National Optical Astronomy Observatories, which are operated by the Association of Universities for Research in Astronomy (AURA) under cooperative agreement with the National Science Foundation.

To register the optical and radio images, accurate positions of stars measured in the extragalactic reference frame are required which should be visible in an optical image that also shows the galaxies G1 and G2. An *I*-band CCD frame of the B2114+022 field was obtained with the NOT in 1996 August 10. On this frame there are seven reference stars from the list of those measured with the Carlsberg Automatic Meridian Circle (Dafydd Wyn Evans, private communication). The Starlink astrometric package GAIA was used to transfer the astrometric calibration to the CCD image; the nominal accuracy of the Carlsberg star positions ranges from  $\pm 0.06$  to  $\pm 0.16$  arcsec. The positions derived for the galaxies G1 and G2 are given in Table 4. Using this astrometry we have superimposed the radio contours derived from the MERLIN 5-GHz map on to the *HST H*-band image. The resulting combined optical + radio image is presented in Fig. 1, with an estimated registration error of 0.1 arcsec. It may be noted that the radio component D coincides with a very faint feature in the *HST H*-band picture. This feature arises from a *single pixel* in the *HST* frame which also shows up in the NICMOS pictures we have of other lensed systems.

## 4 DISCUSSION

### 4.1 B2114+022 as a lensed system

B2114+022 is unique among the  $\sim 15000$  objects of JVAS+CLASS. Normally the presence of four such flat-spectrum radio components within a few arcsec of each other would be taken as very strong evidence that we are dealing with a four-image gravitational lens system (e.g. Schneider, Ehlers & Falco 1992) since each individual radio component has the radio spectrum (Fig. 3) that we would expect from a nuclear radio core.<sup>3</sup> Moreover, the detection of a luminous galaxy (plus a companion) within an arcsec of the radio components is expected in a lensing situation. However, the four-image hypothesis is difficult to sustain. Simply finding a lens model to fit the configuration has proved elusive. In addition, there are the differences in radio spectra and VLBI sub-structures of the components which should all be similar in a quad lensed system. Components A and D have radio spectra and surface brightnesses similar to each other; B and C also have similar spectra and surface brightnesses, but different from A and D.

We therefore believe that B2114+022 must be a two-image gravitational lens system. The chain of argument which supports this conclusion is as follows.

(i) Components A and D have similar compact (mas) radio structures and similar flat radio spectra.<sup>4</sup> The chance of finding two independent sources with such similar properties, and with a potential lensing galaxy between them, is exceedingly remote.

(ii) We would anyway expect component A to be lensed by G1. From its radio properties A is almost certainly the core of an active galaxy. Since no optical/infrared emission has been detected, it must be at a high redshift, certainly greater than that of G1. But G1 is a luminous elliptical galaxy which should be capable of producing multiple images and A (even after some gravitational deflection from its true position) lies only  $\sim 0.4$  arcsec from its

<sup>3</sup> Compact Symmetric Objects (CSOs) also have two flat spectrum components but they have typical separations around 10 mas, not  $\sim 1$  arcsec.

<sup>4</sup> Given the constraint provided by the shape of the spectrum of the sum of the components shown in Fig. 3, all four components must either have flat spectra or a low-frequency turnover.

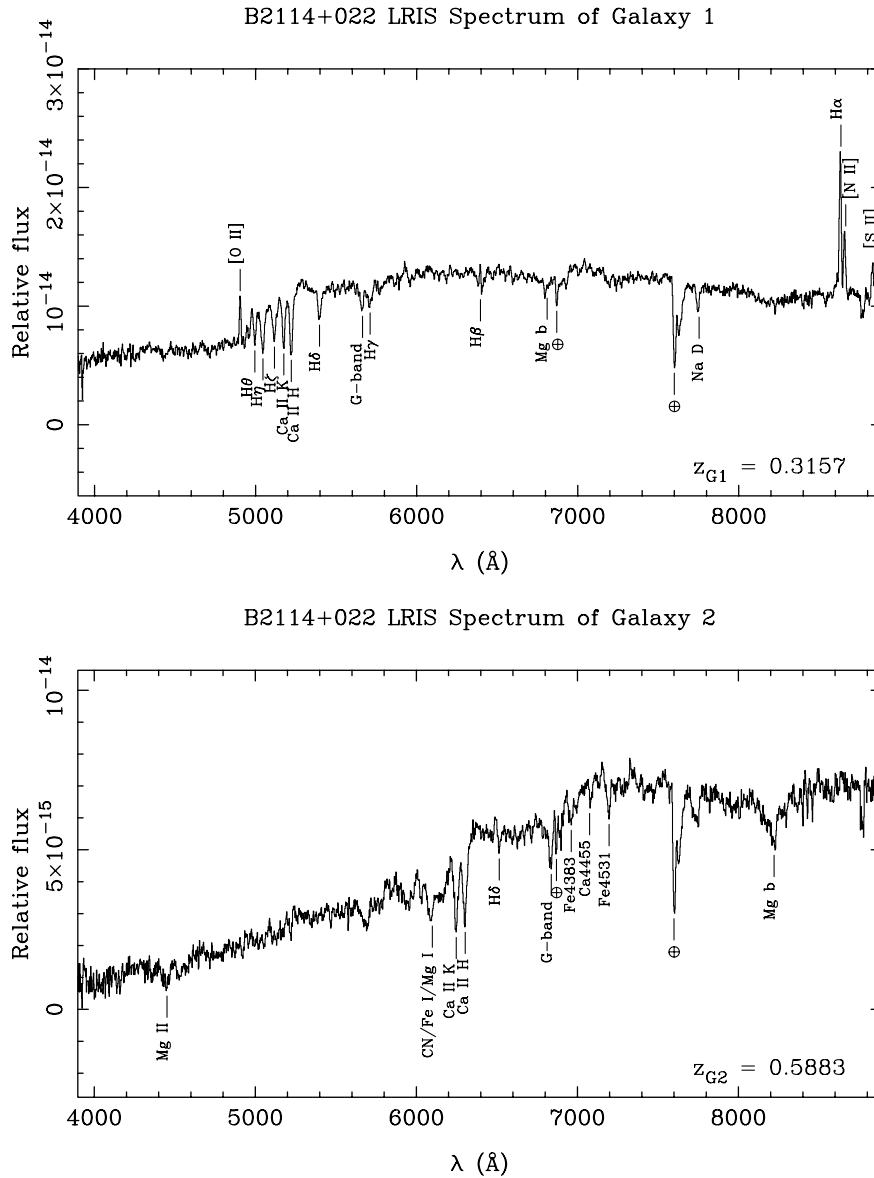


**Figure 4.** The Keck spectra taken of the two galaxies (G1 – top and G2 – bottom) that lie in the field of B2114+022 (Fig. 1). Their spectra give the unambiguous redshifts:  $z_{G1} = 0.3157 \pm 0.0003$  and  $z_{G2} = 0.5883 \pm 0.0003$ .

**Table 4.** Astrometric results. The optical positions are derived from the NOT CCD image calibrated with seven reference stars from the Carlsberg Meridian Circle and have an accuracy  $\sim 0.1$  arcsec. The radio positions are from VLA 8.4 GHz observations and have an accuracy of  $\sim 0.02$  arcsec.

| Component | Right Ascension(J2000) | Declination(J2000) |
|-----------|------------------------|--------------------|
| G1        | 21 16 50.781           | 02 25 46.30        |
| G2        | 21 16 50.791           | 02 25 47.54        |
| A         | 21 16 50.744           | 02 25 46.26        |
| B         | 21 16 50.756           | 02 25 46.59        |
| C         | 21 16 50.769           | 02 25 46.31        |
| D         | 21 16 50.896           | 02 25 47.42        |

centre. Chae et al. (2001) estimate the Einstein radius of G1 as a function of velocity dispersion for an SIS model and show that the impact parameter of A is likely to be smaller than the Einstein radius of G1. Therefore A should be multiply imaged. Component D is the obvious second image.

There appear to be two alternatives within this double-image scenario: either the components B and C are unlensed (perhaps associated with the lensing galaxy itself) or the lensed object has two components, both of which are doubly imaged. For the latter it has proven difficult to find a combination of source structure and lens mass model to produce the observed radio component configuration. The main problem is to simultaneously produce the wide separation of A and D and the small separation of B and C. We therefore argue that B and C are unlensed and are associated with the galaxy G1. In this picture G1, assisted by strong shear from G2, gravitationally lenses a compact background object of unknown redshift to produce images A and D.

We now explore single-plane mass models with the primary aim of showing that a lensing hypothesis is at least tenable. More detailed single-plane and double plane models are explored in the follow up paper by Chae et al. (2001). The redshift of the lensed object is unknown but probably in excess of 2.0 (see Section 4.3). Since varying the source redshift in the modelling only changes the required velocity dispersion for the lens, in the following we will

assume for convenience that the redshift is 2.0. Because of the nearly axisymmetric surface brightness distribution of the primary lens galaxy (G1), we first attempt to model it as a singular isothermal sphere (SIS; e.g. Kormann, Schneider & Bartelmann 1994) plus external shear, caused by the secondary lens galaxy G2. This model is clearly oversimplified, because (i) the surface brightness distribution might not accurately trace the mass distribution and (ii) galaxy G2 lies at a different redshift and has an angular separation from galaxy G1 such that its convergence is probably not negligible and its shear not constant from images A to D.

Five constraints on the simple model come from the image positions and their flux-density ratio. There are, however, also five free parameters: the velocity dispersion of galaxy G1 (1), the position angle and strength of the external shear (2) and the position of the source (2). In general our model will therefore exactly match the observed constraints and no statistical conclusions can be drawn from it. We place the SIS mass distribution at the surface brightness peak of galaxy G1, which constrains its position with respect to the radio structure to within 0.1 arcsec accuracy. We use a flux-density ratio A/D of 3.0, which lies in the middle of the range of 2.3–3.7 found from Table 3. A major complication with this model is that the source position tends to lie within the cusp of the diamond caustic, thus creating a quad and not a double, as observed. This problem cannot be overcome by either changing the flux-density ratio or moving G1 within the 0.1 arcsec box allowed by the astrometric uncertainty, but requires a significantly larger positional shift. All SIS models require an external shear of approx. 0.45 with a PA of approximately  $-30^\circ$ . Both the direction and strength of the external shear are unlikely to be the result of galaxy G2 alone.

An alternative is to assume that G2 has negligible influence and model G1 as a singular isothermal ellipsoid (SIE; Kormann et al.

1994) without external shear. As with the external shear model this one has two additional parameters (i.e. PA and flattening) compared to an SIS mass model. The number of degrees of freedom are therefore zero as well, allowing for a ‘perfect’ fit to the observed constraints. Placing the SIE mass distribution on the same position as before, we find a solution with an axial ratio and PA of  $0.23^\circ$  and  $-34^\circ$ , respectively. A velocity dispersion of  $248 \text{ km s}^{-1}$  is found, assuming the definition in Kormann et al. (1994) and a source redshift of 2.0. We use  $\Omega_m = 0.3$ ,  $\Omega_\Lambda = 0.7$  and  $H_0 = 65 \text{ km s}^{-1} \text{ Mpc}^{-1}$ . For this particular model, shown in Fig. 5, the source lies just outside the cusp in a region where the magnification of image A is greatly enhanced, consequently only a double is created. However, the flattening of the mass distribution is very large (equivalent to a large internal or external shear). In addition the PA does not align with the direction of G2 suggesting the latter is not the ‘sole’ cause of this large shear.

Clearly, both simple models are unsatisfactory, although they illustrate that both the image positions and flux density ratio can be recovered to rough first order within the lensing hypothesis. A more realistic multi-plane lens model is presented in (Chae et al. 2001).

## 4.2 The radio properties of the components

The radio components B and C themselves present a puzzle, irrespective of whether they are lensed or not. The spectra of B and C peak at about 5 GHz but the VLBI observations show that they contain no unresolved mas-sized components. Based both on synchrotron/inverse Compton theory and a wealth of observational data (e.g. Readhead 1994), radio components with flat or peaked spectra are expected to have peak brightness temperatures of  $\sim 10^{11} \text{ K}$ . In the case of components B and C in B2114+022 this would imply that they should contain dominant regions of angular size  $\sim 0.2 \text{ mas}$ . By contrast, they appear to have sizes of  $\sim 20 \text{ mas}$ . The only way out of this dilemma is to presume that, during the propagation of the radio emission from source to observer, either the spectra or the sizes of B and C have been modified. Changing the size (e.g. by scattering) seems unlikely as the information we have suggests that component sizes are not very different at 1.6 and 5 GHz whereas, if scatter broadening were happening, the sizes of the components should scale roughly as  $\lambda^2$ ; i.e. the 1.6-GHz sizes should be factor of nine larger than the 5-GHz sizes. Could the spectrum of the emission have been modified by free–free absorption as the radiation propagates through the galaxy G1? It is known that the supernova remnants in M82 suffer free–free absorption (Wills, Pedlar & Muxlow 1998) and we have already pointed out that the optical spectrum of G1 is that of a post-starburst galaxy resembling that of M82. Thus, given that the lines of sight to B and C pass within 2 kpc of the centre of G1, it is possible that radiation propagating through G1 could be free–free absorbed. This would resolve the size puzzle since the emission from B and C could then have an intrinsically steep spectrum and then the argument for high brightness temperatures goes away. This mechanism could work with the emission from B and C originating either within G1 or from behind it. If free–free absorption occurs, the similarity of the spectra of B and C is surprising given that they pass through very different parts of G1. Thus we are not entirely happy with this free–free absorption explanation, but find it difficult to think of a better alternative.

If B2114+022 is a two-image lens system, components B and C are physically associated with the Galaxy G1. We are, however,

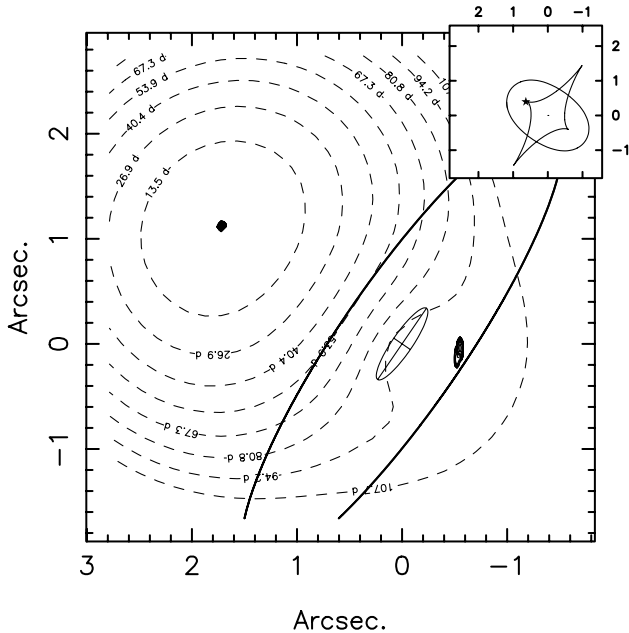


**Figure 5.** The time delay surface (dashed contours labelled in days) for a simple isothermal ellipsoid lens model for B2114+022. Lensed images form at extrema in the time delay surface and their positions are indicated by continuous contours. The position of the lensing galaxy is marked by the small ellipse and the critical curve is the large ellipse. The caustic curves are shown in the insert.

faced by another problem; most radio sources have the lobes roughly symmetrically disposed with respect to the host galaxy but our astrometry does not position G1 between B and C. We cannot completely discount the possibility that the astrometry is wrong but it would require a  $3\sigma$  error to put G1 between B and C. It is thus unlikely that B and C are conventional radio lobes powered by jets emanating from G1. The astrometric errors would allow C to be coincident with G1 and thus C could be a radio core and B a knot in a one-sided radio jet. However, the high-resolution radio map of C (Fig. 2) indicates that its structure is unlike that of most known nuclear radio components. An alternative possibility is that the emission might be associated directly with the starburst activity in G1 as it is in M82 (Muxlow et al. 1994) and Arp220 (Lonsdale, Lonsdale & Diamond 1998). The fact that the emission appears extended and free-free absorbed fits this idea but, as in the case of the radio lobe hypothesis, the lack of symmetry of the radio emission with respect to G1 is a problem.

### 4.3 The nature of the lensed object

The complete absence of optical/infrared emission from the lensed images A and D is surprising. In all the other 18 JVAS/CLASS lens systems the lensed object is detected in the *HST I* and/or *H* images. Perhaps the lack of detectable emission from A is not surprising given the starburst nature of G1 and the fact that its projected distance is within 2 kpc of the nucleus of G1. We might expect such a line of sight to be heavily obscured as happens for example in the lens systems B0218+357 (Jackson, Xanthopoulos & Browne 2000) and B1933+503 (Marlow et al. 1999). However, image D is more than 2 arcsec from G1 and thus extinction seems particularly unlikely. The detection limit on D is  $I \geq 25$  and  $H \geq 23$ . If the lensed object is a galaxy, even if it contains very little optical AGN emission, we would still expect to detect the light from the host galaxy, unless we are dealing with a very high redshift and/or low-luminosity system. Let us take an extreme case and assume that the host galaxy has a brightness of  $\sim 0.2L^*$ . This will be magnified by a factor of 2–3 (Chae et al. 2001) in the lens, say to  $\sim 0.6L^*$ . Even such a sub-luminous galaxy should be detectable out to a redshift of  $\sim 2.5$  in the *HST* images.

## 5 CONCLUSIONS

We are confident that B2114+022 is a gravitational lens system with the galaxy G1 being the primary lens. The lensed images are the radio components A and D. The reasons for our confidence are that (1) even a simple lens model can reproduce to first order the separation of A and D and their flux density ratio and that (2) the compact radio structure and similar flat radio spectra of A and D leave no obvious alternative explanation. Component A lies so close to G1 that it should be multiply imaged and D is an obvious candidate for a lensed image.

The nature of the remaining radio emission which we believe to be associated with G1 (i.e. the components B and C) is still obscure. There are problems with the idea that they are normal radio lobes or even that one is a core and the other part of a jet. It also seems likely that free-free absorption occurring in G1 is needed to produce turn-overs in otherwise steep radio spectra of radio components B and C. This enables us to reconcile the presence of extended radio structure in radio components which have apparently GHz-peaked radio spectra.

The fact that the lens in the B2114+022 system is a starburst galaxy is also of potential interest. There are radio components

behind it and/or within it and this opens up the possibility of probing the medium of the galaxy by studying the propagation effects as radiation passes through it. In addition, we speculate that the radio components B and C might themselves be associated with the starburst activity. If this is the case it suggests that starbursts may be under-represented in low-frequency ( $\leq 1.4$  GHz) radio catalogues simply because the radio emission associated with the supernovae may suffer strong free-free absorption as in the present case. It would then be surprising if there were not more such objects amongst the 15 000 other JVAS/CLASS flat spectrum radio sources. The way to find them would be with VLBI observations looking for objects with surface brightnesses much less than expected on the basis of synchrotron self-absorption theory.

## ACKNOWLEDGMENTS

PA acknowledges the research grants by the Fundação para a Ciência e a Tecnologia (formerly Junta Nacional de Investigação Científica e Tecnológica) Ciência/Praxis XXI BD 2623/93-RM and Praxis XXI BPD 9985/96 and also support for this research by the European Commission under contract ERBFMGECT 950012. Part of this work has been supported by the European Commission, TMR Programme, Research Network Contract ERBFMRXCT96-0034 ‘CERES’. We thank Dafydd Wyn Evans for providing the vital Carlsberg astrometric positions, Andy Biggs for his help with the diagrams, Kyu-Hyun Chae for useful discussions and an anonymous referee for helpful comments.

This research used observations with the *Hubble Space Telescope*, obtained at the Space Telescope Science Institute, which is operated by Associated Universities for Research in Astronomy Inc. under NASA contract NAS5-26555. The Very Large Array and the Very Long Baseline Array are operated by Associated Universities for Research in Astronomy Inc. on behalf of the National Science Foundation. We thank the W. M. Keck foundation for the generous grant that made the W. M. Keck Observatory possible. MERLIN is operated as a National Facility by JBO, University of Manchester, on behalf of the UK Particle Physics & Astronomy Research Council.

## REFERENCES

- Augusto P., 1996, PhD thesis, Univ. Manchester
- Augusto P., Wilkinson P., Browne I., 1998, MNRAS, 299, 1159
- Browne I. W. A., Patnaik A. R., Wilkinson P. N., Wrobel J. M., 1998a, MNRAS, 293, 257
- Browne I. W. A. et al., 1998b, in Bremer M., Jackson N., Perez-Fournon I., eds, *Observational Cosmology with the new radio surveys*. Kluwer Academic Publishers, Dordrecht, p. 305
- Chae K.-H., Mao S., Augusto P., 2001, MNRAS, 326, 1015
- Dressler A., Gunn J., 1983, ApJ, 270, 7
- Hewitt J. N., Turner E. L., Lawrence C. R., Schneider D. P., Brody J. P., 1992, AJ, 104, 968
- Jackson N., Xanthopoulos A., Browne I., 2000, MNRAS, 311, 389
- Kennicutt R. C., 1992, ApJS, 79, 255
- King L. J., Browne I. W. A., Muxlow T. W. B., Narasimha D., Patnaik A. R., Porcas R. W., Wilkinson P. N., 1997, MNRAS, 289, 450
- King L. J., Browne I. W. A., Marlow D. R., Patnaik A. R., Wilkinson P. N., 1999, MNRAS, 307, 225
- Kormann R., Schneider P., Bartelmann M., 1994, A&A, 284, 285
- Lonsdale C. J., Lonsdale C. J., Diamond P. J., 1998, ApJ, 493, L13
- Marlow D., Browne I., Jackson N., Wilkinson P., 1999, MNRAS, 305, 15
- Muxlow T., Pedlar A., Wilkinson P., Axon D., Sanders E., de Bruyn A., 1994, MNRAS, 266, 455
- Oke J. B., 1990, AJ, 99, 1621

- Oke J. B. et al., 1995, *PASP*, 107, 375  
Patnaik A. R., Browne I. W. A., Wilkinson P. N., Wrobel J. M., 1992a, *MNRAS*, 254, 655  
Patnaik A. R., Browne I. W. A., Walsh D., Chaffee F. H., Foltz C. B., 1992b, *MNRAS*, 259, 1P  
Patnaik A. R., Browne I. W. A., King L. J., Muxlow T. W. B., Walsh D., Wilkinson P. N., 1993, *MNRAS*, 261, 435  
Readhead A. C. S., 1994, *ApJ*, 426, 51  
Schneider P., Ehlers J., Falco E. E., 1992, *Gravitational Lenses*. Springer-Verlag, Berlin  
Shepherd M. C., Pearson T. J., Taylor G. B., 1994, *BAAS*, 26, 987  
Wilkinson P. N., Browne I. W. A., Patnaik A. R., Wrobel J. M., Sorathia B., 1998, *MNRAS*, 300, 790  
Wills K. A., Pedlar A., Muxlow T. W. B., 1998, *MNRAS*, 298, 347  
Xanthopoulos E. et al., 1998, *MNRAS*, 300, 649

This paper has been typeset from a  $\text{\TeX/L\AA\TeX}$  file prepared by the author.